18. H. Oraizi and S. Hedayati, Miniaturized UWB monopole microstrip antenna design by the combination of Giusepe Peano and Sierpinski carpet fractals, IEEE Antennas Wireless Propag Lett 10 (2011), 67–70.
19. R. Kumar and K. Sawant, On the design of inscribed triangle non-concentric circular fractal antenna, Microwave Opt Technol Lett 52 (2010), 2696–2699.
20. A. Azari and J. Rowhani, Ultra wideband fractal microstrip antenna design, Prog Electromagn Res C 2 (2008), 7–12.
21. C. Mahatthanajatuphat, P. Akkaraekthalin, S. Saleekaw, and M. Krairiksh, A bidirectional multiband antenna with modified fractal slot fed by CPW, Prog Electromagn Res 95 (2009), 59–72.
22. R. Kumar, M. Dhananjay, and K. Kailas Sawant, On the design of inscribed triangle circular fractal antenna for UWB applications, AEU Int J Electron Commun 66 (2012), 68–75.
23. D. Li and J.F. Mao, Sierpinskized Koch-like sided multifractal dipole antenna, Prog Electromagn Res 130 (2012), 207–224.
24. Ansoft Corporation, HFSS, High frequency structure simulator version 11, Finite element package, Ansoft Corporation, Available at: http://www.ansoft.com.
25. CST Inc., CST microwave studio suite 2011, CST Inc., Wellesley Hills, MA, 2007.
26. C.A. Balanis, Antenna theory: Analysis and design, 3rd ed., Wiley, Hoboken, NJ, India Edition, 2012.
27. Y.H. Li and J.T. Lue, Dielectric constants of single-wall carbon nanotubes at various frequencies, J Nanosci Nanotechnol 7 (2007), 1–4.
28. K. Mohit, V.R. Gupta, N. Gupta, and S.K .Rout, Structural and microwave characterization of $Ni_{0.2}Co_xZn_{0.8\text{-}x}Fe_2O_4$ for antenna applications, Ceram Int 40 (2014), 1575–1586.
29. R. Ghatak, B. Biswas, A. Karmakar, and D.R. Poddar, A circular fractal uwb antenna based on descartes circle theorem with band rejection capability, Prog Electromagn Res C 37 (2013), 235–248.
30. N.M. Sahar, M.T. Islam and N. Misran, Analysis of fractal antenna for ultra wideband application, Res J Appl Sci Eng Technol 7 (2014), 2022–2026.
31. F.B. Zarrabi, A.M. Shire, M. Rahimi, and N.P. Gandji, Ultra-wideband tapered patch antenna with fractal slots for dual notch application, Microwave Opt Technol Lett 56 (2014), 1344–1348.
32. M. Ding, R. Jin, J. Geng, and Q. Wu, Design of a CPW-fed ultrawideband fractal antenna, Microwave Opt Technol Lett 49 (2007), 173–176.
33. H. Fallahi and Z. Atlasbaf, Study of a class of UWB CPW-fed monopole antenna with fractal elements, IEEE Antennas Wireless Propag Lett 12 (2013), 1484–1487.
34. X. Begaud, Ultra wideband antennas, Wiley, New Jersey, 2011.
35. The European table of Frequency Allocations and Applications, ERC Report 25, May 2014.

A NOVEL VIA-FREE MICROSTRIP BALANCED-TO-BALANCED DIPLEXER FOR NARROW-BAND APPLICATIONS

Arcesio Arbelaez-Nieto, Jose-Luis Olvera-Cervantes, Johanny-Alberto Escobar-Pelaez, and Alonso Corona-Chavez
Department of Electronics, INAOE, Puebla, Mexico; Corresponding author: arbelaez@inaoep.mx

Received 10 July 2014

ABSTRACT: *In this article, a new type of microstrip vias-free balanced-to-balanced diplexer suitable for narrow-band applications is presented. The structure of the balanced diplexer is based on two balanced bandpass filters designed for f1=1.1 GHz and f2=1.8 GHz and two transmission lines used to satisfy the open circuit conditions required in the diplexer's design. This diplexer exhibits good common-mode rejection ratio better than 40 dB at the passbands. The attenuation is better than 35 dB at the rejection bands. The isolation between output ports is better than 50 dB. Simulated and experimental results are compared with good agreement. The diplexer is easy of fabricate and integrate with others planar balanced devices.* © 2015 Wiley Periodicals, Inc. Microwave Opt Technol Lett 57:567–570, 2015; View this article online at wileyonlinelibrary.com. DOI 10.1002/mop.28902

Key words: *diplexer; differential signals; common mode; balanced bandpass filter; common mode rejection ratio*

1. INTRODUCTION

Differential signals have taken great importance due to the high tolerance to interferences and low levels of radiation compared to single-ended signal circuits. Also, new devices such as: amplifiers [1], antennas [2], mixers [3], and diplexers [4], are built using differential signal to reduce the common mode noise.

A balanced-to-balanced diplexer is a device with a differential input port and two differential output ports with two separate frequency bands. These devices are important in systems where the signal from a balanced device (e.g., a differential antenna) must be separated to feed two differential devices (e.g., differential amplifiers).

Several diplexers are found in the literature. Almost all of them have single-ended terminals [5, 6], but these are not appropriate for balanced systems. Some differential diplexers are found in Refs. 7–10. In Ref. 7, a balanced-to unbalanced diplexer is shown. However, it is not possible have a balanced device at the output ports.

Additionally, a diplexer with high selectivity and common-mode suppression is presented in Ref. 8. For this device there are two possible configurations in which full support for balanced devices at both ends (input and output) is possible.

A diplexer with full support for balanced devices is described in Ref. 9. This diplexer is based on directional bandpass filters. The prototype has a good noise attenuation in common-mode and it is easy of fabricate on microstrip technology but is not suitable for narrow-band applications.

Moreover, a narrow-band balanced-to-balanced diplexer without extra matching network is proposed in Ref. 10 but requiring via holes which are not suitable for two-dimensional fabrication [5]. The diplexer was designed for 2.45 and 3.6 GHz. It is based on two filters composed of two quarter wavelength resonators and source-load short-ended feedlines. The diplexer exhibits good CMRR, high selectivity but poor isolation between the output ports (only 33 dB).

In this article, a balanced-to-balanced planar microstrip via free diplexer is presented. The frequencies used are 1.1 and 1.8 GHz and the passband filters are two balanced bandpass filters (BBPF) at the corresponding frequencies. The proposed diplexer presents good CMRR, high selectivity, compact size, good isolation between differential ports, and ease of integration with other planar technology because this can be built on the same substrate as other planar devices and vias holes are not required.

2. DIPLEXER DESIGN

The layout and the dimensions of the proposed diplexer for the Rogers RO4003C substrate, with relative permittivity $\varepsilon_r = 3.38$ and 0.81 mm dielectric thickness, are shown in Figure 1. The proposed diplexer requires two balanced bandpass filters (BBPF1 and BBPF2) with central frequencies of 1.1 and 1.8 GHz and two 50 Ω coupling transmission lines (Line 1 and

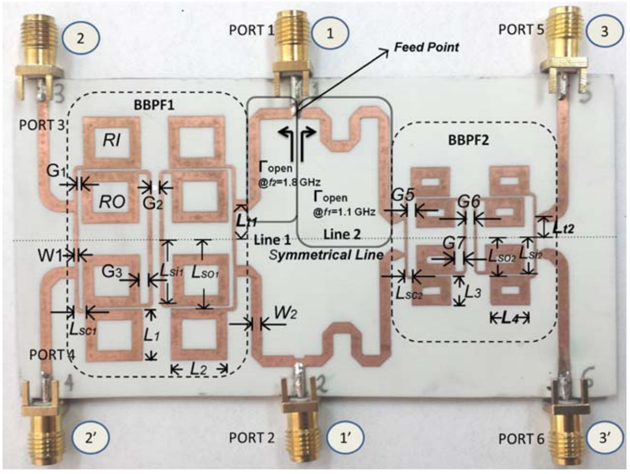

Figure 1 Schematic of the proposed diplexer, $G_1 = 0.84$ mm, $G_2 = 1.57$ mm, $G_3 = 1.65$ mm, $G_5 = 1.52$ mm, $G_6 = 1.33$ mm, $G_7 = 1.44$ mm, $L_{t1} = 5.4$mm, $L_{t2} = 2.97$ mm, $L_1 = 8.6$ mm, $L_2 = 9.6$ mm, $L_3 = 4.8$ mm, $L_4 = 6.6$ mm, $W_1 = 0.45$ mm, $W_2 = 1.8$ mm, $L_2 = 1.8$ mm, $L_{sc1} = 1.72$ mm, $L_{si1} = 10.78$ mm, $L_{so1} = 11.53$ mm, $L_{sc2} = 1.15$ mm, $L_{si2} = 6.25$ mm, $L_{so2} = 6.5$ mm. [Color figure can be viewed in the online issue, which is available at wileyonlinelibrary.com]

Line 2). To design each filter [11], the first step is to devise two resonators composed of two closed-loop transmission lines of characteristic impedance ZCL= 50 Ω and electrical length of 53.13° at the central frequency.

The second step is to establish the external and mutual coupling coefficients. According to the specification of a four-pole Butterworth low pass prototype with FBW = 10% the design parameters are $Q_{e1}^d = Q_{e4}^d = 7.654, M_{12}^d = M_{34}^d = 0.084$, and $M_{23}^d = 0.0541$where Q_{e1}^d and Q_{e4}^d are the required external couplings coefficients for the first and last resonators and M_{ij}^d are the differential mode mutual coupling coefficients between resonators.

The third step is to obtain the practical dimensions of the filter corresponding to the calculated coupling coefficients using a full wave simulator.

The transmission line 1 (Fig. 1) is calculated to achieve an open circuit at the feed point at $f2 = 1.8$ GHz for the differential mode. This condition is reached using a transmission line (delay line) with an electrical length $\theta 1 = 112.7°$. In the same manner, Line 2 is calculated with a length ($\theta 1 = 62.6°$) to obtain an open circuit at $f1 = 1.1$ GHz. The filters are combined with the transmission line to obtain a balanced diplexer as shown in Figure 1. Clearly, in differential mode operation, a virtual short circuit is generated in the symmetrical line due to the circuit symmetry.

3. SIMULATED AND EXPERIMENTAL RESULTS

Measured *S*-parameters in differential and common modes were obtained using a two port vector network analyzer (VNA). To obtain the six ports *S* matrix it was necessary to take several sets of two ports measurements and then the complete matrix was built. The element *Sij* of the *S*-parameter matrix is obtained using the VNA connected to two ports of the diplexer (Port *i* and Port *j*), while the remaining ports are connected to 50 Ω loads, for example, when Port 1 and Port 2 are used for the measurements, four loads of 50 Ω are required in the remaining ports. The three differential and common mode *S*-parameters were obtained from six port *S*-parameters as is defined in Ref. 12. The area of the proposed diplexer is $0.44\lambda_{gl} \times 0.24\lambda_{gl}$ where

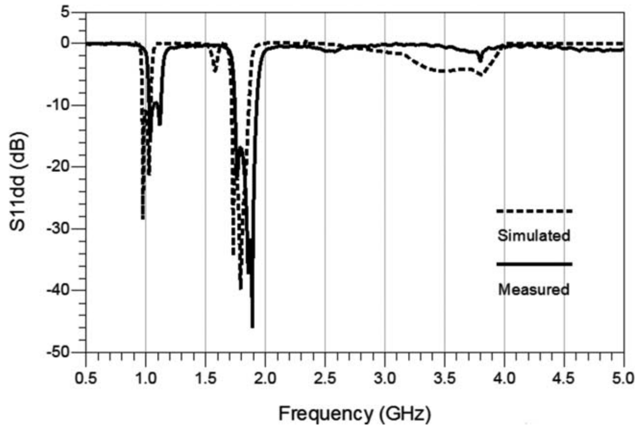

Figure 2 Simulated and measured differential S_{11}.

λ_{gl} is the guided wavelength of 50 Ω line on the substrate at the center frequency of the lower passband. This is smaller than the circuit presented in Ref. 10 as the circuits occupy an area of $0.62\lambda_{gl} \times 0.62\lambda_{gl}$ at their lower passband. Additionally, it is possible to obtain a good performance when both bands are separated by a large or small frequency spacing due to the performance depends on the individual characteristics of the filters. A good filter's selectivity is required for small frequency spacing and a free spurious band is important for a large frequency spacing.

3.1. Differential Mode Response

In this section, the comparisons between simulations and measurements are shown. In Figure 2, simulated and measured return losses are shown. The return losses are better than 10 dB for the

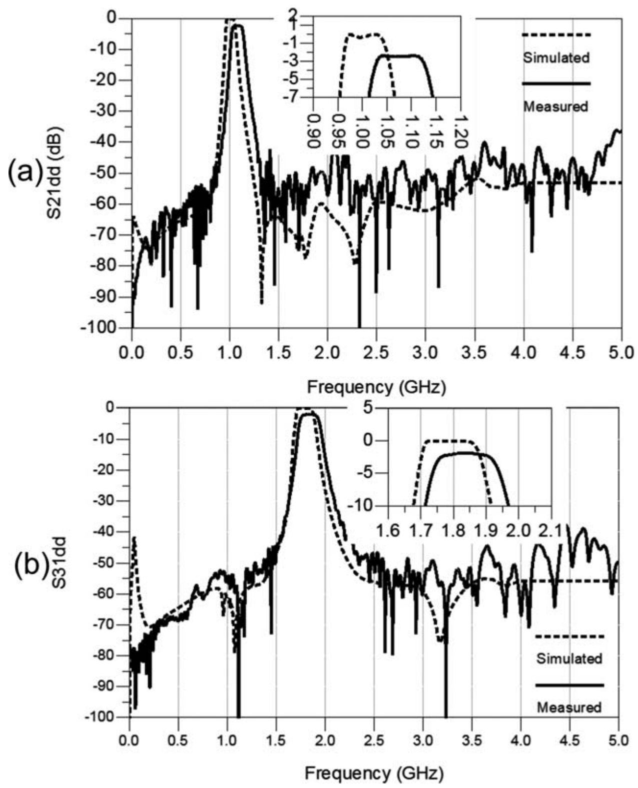

Figure 3 Simulated and measured differential mode: (a) S_{21} and (b) S_{31}.

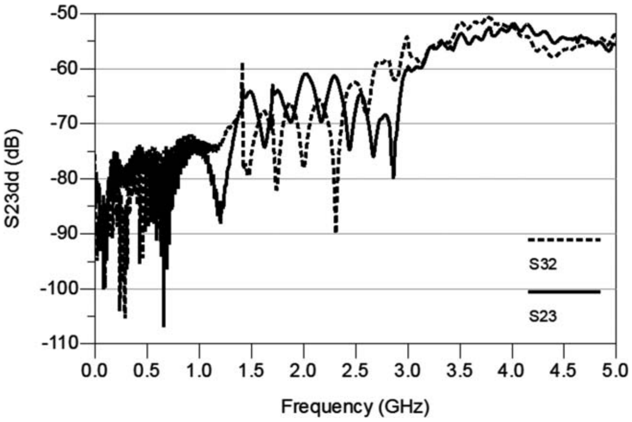

Figure 4 Isolation under differential mode operation.

first passband and about 20 dB for the second band. This is explained as the second filter was optimized more efficiently. In Figure 3, $S21dd$ and $S31dd$ are shown. In Figure 3(a), the measured central frequency in the first BBPF is 1.079 GHz and the fractional bandwidth is 11.22%. In Figure 3(b), the second BBPF has a measured central frequency of 1.843 GHz and the fractional bandwidth is 10.96%. Also, the insertion loss is close to 2.3 and 1.85 dB for the BBPF1 (S_{21dd}) and BBPF2 (S_{31dd}), respectively.

Also, in Figure 3, it can be seen that the insertion losses under differential mode operation are better that 40 dB up to $4.7f1$ between Port 1 and Port 2 and better that 39 dB up to $2.6f2$ between Port 1 and Port 3, respectively. Which is better than the ones reported in the literature. In Ref. 10, the insertion losses are better that 40 dB up to only $2.5f1$ and close to only 27 dB in the rejection band between Port 1 and Port 3, we can

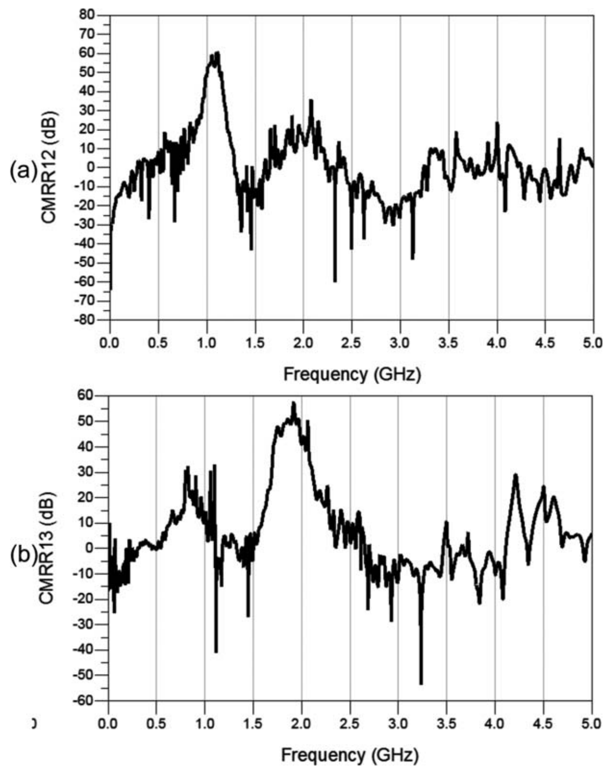

Figure 5 Measured CMRR: (a) CMRR between Port 1 and Port 2; (b) CMRR between Port 1 and Port 3.

TABLE 1 Comparison with Diplexer in []

	f (GHz)	BW (%)	CMRR (dB)	DM Isolation (dB)	DM Attenuation (dB)
[10]	2.45, 3.6	6, 3	>40	>33	>43
This	1, 1.8	11.22, 10.96	>45	>50	>35

say that the proposed diplexer exhibits better attenuation out of band than the other one in Ref. 10. Also, the isolation between Port 2 and Port 3 is shown in Figure 4. The passband isolation is better than 50 dB.

3.2. Common-Mode Rejection Ratio

The parameter used to determine the ability to suppress the common-mode noise is the CMRR, which is defined as follows [13]

$$\mathrm{CMRR}_{1i} = -20\log\frac{|S_{i1dd}|}{|S_{i1cc}|}, \tag{1}$$

When CMRR approaches to infinity the diplexer is near to ideal case and the common-mode suppression is high. In this case, the CMRR is better than 50 dB in the first band and better than 40 dB in the second band (Fig. 5). All characteristics are summarized in Table 1.

4. CONCLUSION

A miniaturized via-free balanced-to-balanced diplexer for 1.1 and 1.8 GHz has been presented. The structure exhibits high common mode suppression in the bands of interest (CMRR > 45 dB). The isolation between output ports is greater than 50 dB. A good attenuation in rejection bands for the differential mode is reached (>35 dB). This diplexer exhibits a size reduction without requiring vias holes. Additionally, it is possible to obtain a good performance when both bands are separated by large or small frequency spacing. The diplexer is easy to fabricate and integrate with other planar balanced devices. Good agreement between the simulations and measurements has been achieved.

REFERENCES

1. N. Wadefalk, P.S. Kildal, and H. Zirath, A low noise integrated 0.3-16 ghz differential amplifier for balanced ultra wideband antennas, In: Proceedings of the IEEE Compound Semiconductor Integrated Circuit Symposium (CSICS), 2010, pp. 1–4.
2. X.S. Fang, K.W. Leung, E.H. Lin, and R.S Chen, Compact differential rectangular dielectric resonator antenna, IEEE Antennas Wireless Propag Lett 9 (2010), 662–665.
3. X.B. Li, M.J. Zhao, Z.H. Wu, and B. Li, A high-linearity fully-differential mixer, In: Proceedings of the International Conference of Electron Devices and Solid-State Circuits (EDSSC), 2011, pp. 1–2.
4. H.Y. Zeng, G.M. Wang, D.Z. Wei, and Y.W. Wang, Planar diplexer using composite right-/left-handed transmission line under balanced condition, Electron Lett 48 (2012), 104–106.
5. V. Mishra, R.K. Chaudhary, K.V. Srivastava, and A. Biswas, Compact two poles bandpass filter implemented using via-free composite right/left handed transmission line with radial stubs, In: Proceedings of the 41st European Microwave Conference (EuMC), Manchester, UK, 2011, pp. 571–574.
6. W. Qin and Q. Xue, Design of a planar diplexer based on complementary compact microstrip resonant cell, In: Proceedings of the IEEE Asia Pacific Microwave Conference Proceedings (APMC), Taipei. Taiwan, 2012, pp. 526–528.
7. C.H. Wu, C.H. Wang, and C.H. Chen, A novel balanced-to-unbalanced diplexer based on four-port balanced-to-balanced bandpass filter, In: Proceedings of the 38th European Microwave Conference (EuMC), Amsterdam, The Netherlands, October 2008, pp. 28–31.

8. Q. Xue, J. Shi, and J.X. Chen, Unbalanced-to-balanced and balancedto-unbalanced diplexer with high selectivity and common-mode supression, IEEE Trans Microwave Theory Tech 59 (2011), 2848–2855.
9. H. Lobato Morales, S. Sun Jim, A. Corona Ch'avez, T. Itoh, J.L. Olvera Cervantes, UWB and WLAN microstrip diplexer for differential-mode operation, In: Proceedings of the Microwave Symposium Digest (MTT), IEEE MTT-S International, Montreal, Canada, 2012, pp. 1–3.
10. H. Deng, Y. Zhao, Y. Fu, Y. He, and X. Zhao, High selectivity and CM suppression microstrip balanced BPF and balanced-to-balanced diplexer, J Electromagn Waves Appl 27 (2013), 1047–1058.
11. J.L. Olvera Cervantes and A. Corona Ch'avez, Microstrip balanced bandpass filter with compact size, extended-stopband and common-mode noise suppression, IEEE Microwave Wireless Compon Lett 23 (2013), 530–532.
12. D.E. Bockelman and W.R. Eisenstadt, Combined differential and common-mode scattering parameters: Theory and simulation, IEEE Trans Microwave Theory Tech 43 (1995), 1530–1539.
13. C.H. Wu, C.H. Wang, and C.H. Cheng, Novel balanced coupled-line bandpass filters with common-mode noise suppression, IEEE Trans Microwave Theory Tech 55 (2007), 287–295.

A COMPACT OCTAGONAL-SHAPED FRACTAL UWB ANTENNA WITH SIERPINSKI FRACTAL GEOMETRY

Shrivishal Tripathi,[1] Akhilesh Mohan,[2] and Sandeep Yadav[1]
[1] Centre of Excellence in Information and Communication Technology, Indian Institute of Technology Jodhpur, Jodhpur, Rajasthan, India; Corresponding author: shrivishal@iitj.ac.in
[2] Department of E&EC, Indian Institute of Technology Kharagpur, Kharagpur, West Bengal, India

Received 16 July 2014

ABSTRACT: *In this letter, a compact ultrawideband (UWB) antenna using Sierpinski fractal geometry is presented and its characteristics are investigated. The miniaturization and wideband phenomena are attained due to introduction of Sierpinski fractal geometry in the UWB antenna design. The proposed antenna has a compact dimension of 25 × 16 mm². It exhibits nearly omnidirectional radiation pattern, good return loss with good time domain response in terms of fidelity factor (>0.86) over the entire UWB frequency range. The presented prototype is fabricated and it demonstrates good measured characteristics with the simulated one.* © 2015 Wiley Periodicals, Inc. Microwave Opt Technol Lett 57:570–574, 2015; View this article online at wileyonlinelibrary.com. DOI 10.1002/mop.28901

Key words: *ultrawideband antenna; fractal geometry; Sierpinski; fidelity factor; time-domain analysis*

1. INTRODUCTION

The demand for ultrawideband (UWB) technology system is increased due to its potential applications in indoor communication. The UWB technology requires high data transmission capacity at very low power, large bandwidth, omnidirectional radiation pattern, and high gain in short range communications [1]. However, design of a compact wideband antenna which meets the above requirements is a challenging task. These problems can be resolved by applying Sierpinski fractal geometry in UWB antenna design. The application of fractal geometry in antenna design provides the desired miniaturization and wideband bandwidth because of its self-similarity and space filling properties [2–4]. The space filling properties with multiple iterations helps to increase the effective electrical path length of the antenna [4]. The fractal geometries such as hexagonal shaped [3], Sierpinski snowflake [4], Sierpinski triangle [3, 4], and some other fractal geometry [5, 6] are used to design UWB antenna. All the above fractal antennas show repetition of a small part of the geometry in a self-similar manner, which leads to improvement in antenna characteristics [4]. The discontinuities and bends in the fractal geometry change the current path, which leads to enhance the radiation characteristics [7]. Hence, in this article, we present a promising compact octagonal-shaped fractal UWB antenna using Sierpinski fractal geometry to exploit the wideband and improved radiation property of fractal geometry. The Sierpinski fractal geometry is combined with the octagonal-shaped geometry to increase the effective electrical path length in a smaller area due to its space filling properties. These modifications in the geometry excite additional resonances, which enhances the bandwidth. The optimized antenna has a compact dimension of 25 × 16 mm^2. To provide more insight into the behavior of the antenna, time domain analysis is also carried out. The proposed antenna is fabricated, and the experimental results are also discussed.

2. ANTENNA DESIGN

Figure 1 shows the geometry of the proposed UWB antenna on a rectangular FR4 epoxy substrate ($W \times L$) having a dielectric constant of $\varepsilon_r = 4.4$, loss tangent tan $\delta = 0.023$, and thickness (h) of 1.6 mm. The proposed antenna is simulated and optimized using Ansoft HFSS v.13. The rectangular substrate dimensions show wideband operability and good radiation characteristics [8]. Hence, the rectangular dimension is preferred as

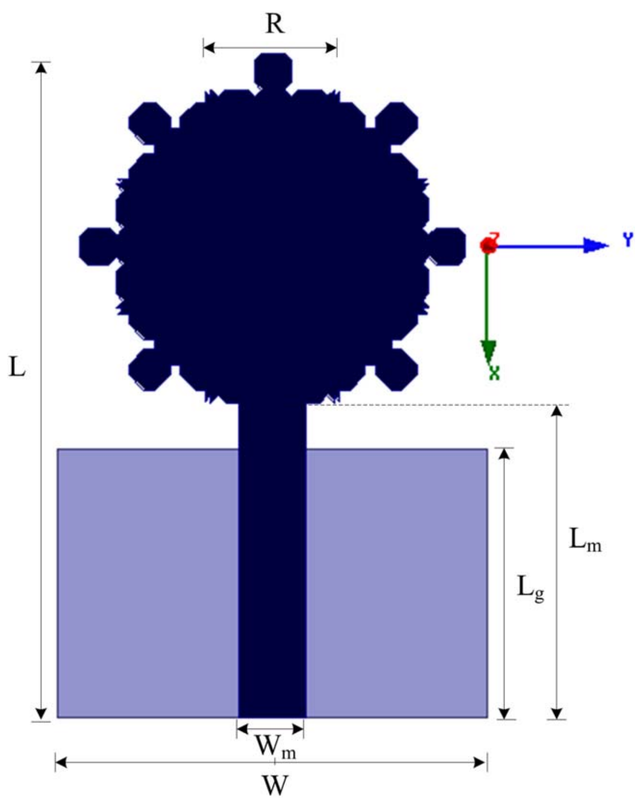

Figure 1 Geometry of proposed fractal UWB antenna. [Color figure can be viewed in the online issue, which is available at wileyonlinelibrary.com]